X- and W-Band Time-Resolved Electron Paramagnetic Resonance Studies on Radical-Excited Triplet Pairs between Metalloporphyrins and Axial-Ligating Nitroxide Radicals

Jun-ichi Fujisawa, Kazuyuki Ishii,† Yasunori Ohba, and Seigo Yamauchi*

Institute for Chemical Reaction Science, Tohoku University, Katahira 2-1-1, Aoba-ku, Sendai 980-77, Japan

Michael Fuhs and Klaus Möbius

Institute of Experimental Physics, Free University of Berlin, Arnimallee 14, D-1000 Berlin 33, Germany

Received: April 1, 1997; In Final Form: June 6, 1997[⊗]

A chemically induced dynamic electron spin polarization (CIDEP) study has been accomplished on radical-excited triplet pairs (RTP) in systems of metalloporphyrins, MgTPP, ZnTPP, and ZnOEP, and pyridine-substituted nitronyl nitroxide radicals, nit-R (R = o-py, m-py, and p-py), by X- (9.5 GHz) and W-band (95 GHz) time-resolved electron paramagnetic resonance (TREPR) in solution. Axial-ligations between the porphyrins and the radicals were ascertained from visible absorption spectra except for the nit-o-py system. The TREPR spectra were composed of two signals, which were assigned to those of the ground (D_0) state of the radical and the excited quartet (Q_1) state of the RTP. These components showed two kinds of CIDEPs in different time regions. The polarizations of the Q_1 state were attributed to radical−triplet pair mechanisms (RTPMs) with singlet and triplet precursors. In the nit-p-py and the nit-m-py systems, the polarizations of the radical were generated via an electron spin polarization transfer (ESPT) from the Q_1 state and the RTPM. The CIDEPs observed for the nit-o-py system were interpreted by ESPT and RTPM with the excited triplet (T_1) porphyrin. From the analysis of the RTPM polarizations, an exchange interaction between the T_1 porphyrin and the radical was found to be ferromagnetic for the nit-p-py system and antiferromagnetic for the nit-m-py and the nit-o-py systems.

Introduction

In recent years, chemically induced dynamic electron spin polarizations (CIDEPs) have been extensively investigated in various systems of radicals (R) and excited triplet (T) molecules by means of time-resolved electron paramagnetic resonance (TREPR), which is a useful technique that enables us to observe transient CIDEP signals of paramagnetic species.[1−6] Stable radicals are well-known to exhibit CIDEP effects due to a radical−triplet interaction, which provides unique information on spin and reaction dynamics in R−T systems.[2−4,6] Two CIDEP mechanisms, a radical−triplet pair mechanism (RTPM)[1−6] and an electron spin polarization transfer (ESPT)[6] have been proposed to interpret generated polarizations. For RTPM, the CIDEP arises from mixings of excited quartet (Q_1) and doublet (D_1) states originating from an exchange interaction ($H_{ex} = -2J\mathbf{S}_T\cdot\mathbf{S}_D$) between R and T. In this mechanism, two types of mixings due to fine structure and hyperfine interactions produce hyperfine-level-independent (net) and level-dependent (multiplet) polarizations, respectively. The polarizations exhibit different signs depending on quenchings of excited singlet and triplet states by radicals such as A + A/E and E + E/A under $J < 0$, respectively.[3,6] These polarizations are inverted to E + E/A and A + A/E under $J > 0$ for the singlet and triplet precursors, respectively. Therefore, analyses of the RTPM polarizations directly provide information about a sign of the exchange coupling parameter J between R and T.

On the other hand, for ESPT the spin polarization originates from the T_1 state via a sublevel-dependent intersystem crossing (isc) between S_1 and T_1. The T_1 polarization is transferred to a radical via the exchange interaction between R and T with conservation of the spin alignment.[6] Thus, the ESPT polarization appears on a radical exhibiting the same polarization of the T_1 state.

Excited quartet (Q_1) and doublet (D_1) states have been studied in several systems of copper−[7,8] and vanadium−porphyrins[7c] and organic radicals[9,10] by means of TREPR, optically detected magnetic resonance (ODMR), and transient absorption spectroscopy. Recently, an EPR signal of a Q_1 state generated from a radical-excited triplet pair (RTP) has been observed in solution [11] and those of Q_1 and D_1 states in a solid[12] by TREPR. Although RTP is a key species in elucidating the interaction between R and T and the CIDEP mechanism,[13] very few CIDEP studies have been reported so far for RTP in solution.

Here, we report on electron spin polarizations of the RTPs in systems of metalloporphyrins and axial-ligating stable radicals by X- (9.5 GHz) and W-band (95 GHz) TREPR in toluene solution. Our objectives are (1) direct observations of the Q_1 and the D_1 states in RTP, (2) interpretations of electron spin polarizations of RTP in fluid solution, and (3) analyses of a sign of an exchange coupling parameter J between R and T. Three kinds of nitroxide radicals, 2-(*R*)-4,4,5,5-tetramethyl-4,5-dihydro-1*H*-imidazol-1-oxy-3-oxide (R = 2-pyridyl, 3-pyridyl, 4-pyridyl) which are abbreviated as nit-o-py, nit-m-py, and nit-p-py, respectively, and metalloporphyrins, MgTPP, ZnTPP, and ZnOEP (TPP = tetraphenylporphyrin; OEP = octaethylporphyrin), were selected and are shown in Figure 1. The T_1 porphyrins examined were reported to exhibit similar zero-field splitting parameters D[14−16] but different polarizations, emissive for MgTPP[14,15a] and absorptive for ZnTPP[15,16] and ZnOEP.[16]

* To whom correspondence should be addressed.
† Present address: Department of Chemistry, Graduate School of Science, Tohoku University, Sendai 980, Japan
⊗ Abstract published in *Advance ACS Abstracts,* August 1, 1997.

S1089-5639(97)01147-X CCC: $14.00

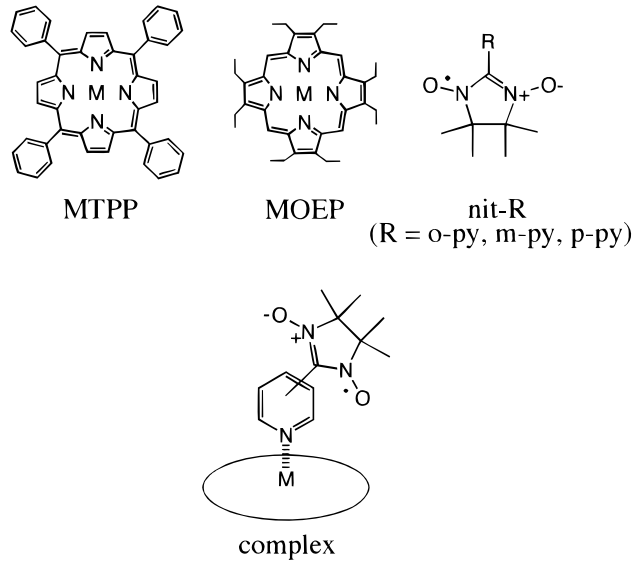

Figure 1. Molecular structures of metalloporphyrins, nitroxide radicals, and the axial-ligated complex.

Experimental Section

MgTPP,[17,19] ZnTPP,[17,18] ZnOEP,[17,18] nit-o-py,[20] nit-m-py,[20] and nit-p-py,[20] were synthesized according to methods described in the literature. H_2OEP was purchased from Aldrich to synthesize ZnOEP. Spectral grade toluene as solvent and pyridine (Wako Pure Chemicals) were used without further purification. The solution was deaerated by repeated freeze−pump−thaw cycles on a vacuum line in all experiments except for UV−vis absorption measurements.

X-band (9.5 GHz) steady-state and time-resolved EPR measurements were carried out using a modified JEOL JES-FE2XG EPR spectrometer. In the TREPR experiments, a transient EPR signal was taken directly from the microwave detector diode without field modulation and fed into a laboratory-built fast amplifier. For TREPR spectra and time profiles, the signal was collected and averaged by a NF BX-531 boxcar integrator and an Iwatsu DM-7200 digital memory, respectively. The W-band TREPR apparatus has been described previously.[21] An OPO laser (MOPO-710 Spectra Physics) pumped by a Nd:YAG laser (GCR 170 Spectra Physics) was employed to excite the samples at various wavelengths in the visible region. In the W-band TREPR experiments, the second harmonics (λ = 532 nm) of a Nd:YAG laser (GCR 170 Spectra Physics) was used to excite the sample. UV−vis absorption spectra were obtained using a Shimadzu UV-240 spectrometer. Transient absorption measurements were performed by using a Nikon G250 monochromator and a Hamamatsu Photonics R928 photomultiplier with a continuous wave Xe lamp (Hamamatsu C4263). All experiments were made at room temperature.

Results and Interpretation

1. Absorption Spectra. Visible absorption spectra of ZnTPP were measured at different concentrations of the nit-p-py radical and are shown in Figure 2a. The spectrum was shifted to the red with addition of nit-p-py, which indicates ligation occurring between ZnTPP and nit-p-py. Figure 2b shows the analyzed spectra of ZnTPP and the complex, where the spectrum of the complex is observed at longer wavelength (ca. 15 nm) and closely resembles that of the ZnTPP−pyridine system.[22] Similar spectral shifts were observed in the systems of nit-m-py, but little shift was observed in the nit-o-py systems. These results indicate directly that the axial ligation of nit-p-py and nit-m-py occurs between the central metal of the porphyrin and the nitrogen atom of the pyridine ring of the radical, as shown in Figure 1. The following equilibrium (1) is achieved

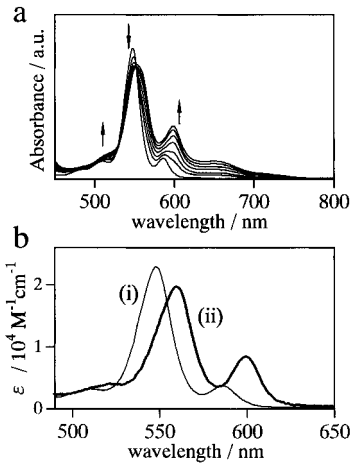

Figure 2. Absorption spectra of (a) ZnTPP with different concentrations of nit-p-py and (b) those of (i) ZnTPP and (ii) the ZnTPP-nit-p-py complex in toluene.

$$\mathrm{MP} + \text{nit-py} \rightleftarrows [\text{nit-py}\cdots\mathrm{MP}] \qquad (\mathrm{M} = \mathrm{Mg}, \mathrm{Zn}) \quad (1)$$

among the species and the equilibrium constants for the ZnTPP, ZnOEP, and MgTPP systems were determined as 5000, 3500, 2500 ± 700 M^{-1}, respectively, from the analysis of the visible absorption spectra at different concentrations of radicals (Figure 2). These values are similar to those reported for the porphyrin−pyridine systems.[22] Accordingly, there are three species, the noncoordinating radical, the uncomplexed metalloporphyrin, and the complex existing in the nit-p-py and the nit-m-py systems. For the nit-o-py system, such a strong axial ligation occurring in nit-p-py and nit-m-py was not observed, probably due to steric hindrance. However, we consider that the weak ligation occurs between the oxygen atom of the radical and Zn of ZnTPP from the spectral shift of phosphorescence observed in the solid phase[23] and the effect of pyridine described in the section 2.

2. Spectra and Decays of CIDEP Signals. *a. X-Band EPR. (1). ZnTPP-nit-p-py System.* A steady-state spectrum of nit-p-py was observed as shown in Figure 3a, showing five peaks (g = 2.0068, A_N = 0.74 mT)[24] due to two equivalent nitrogen atoms of the nitroxide moiety. X-band TREPR spectra observed for the ZnTPP (2 mM) and nit-p-py (5 mM) system are shown in Figure 3b. Under these concentrations, 95% ZnTPP ligates with nit-p-py, giving 1.9 mM complex, 0.1 mM free ZnTPP, and 3.1 mM free nit-p-py. The laser wavelength was selected at 620 nm in order to excite selectively the complex. The signals were emissive at earlier times (0.1−0.2 μs) and turned to be absorptive at later times (0.5−0.6 μs). It was also found that two components of the CIDEP signals were observed as sharp and broad ones in the spectra. We carried out a spectral simulation as shown in Figure 4. The TREPR spectra were simulated with the five Lorentzian peaks based on the EPR parameters of nit-p-py (Figure 3a) and one broad Gaussian peak. The g value and the full width at half-height ($\Delta B_{1/2}$) of the broad signal were determined as 2.0032 ± 0.0005 and 1.8 ± 0.3 mT, respectively. TREPR spectra under the concentrations of 0.5 mM ZnTPP and 0.5 mM nit-p-py are shown in Figure 3c. The spectra observed at 0.1−0.2 and 0.5−0.6 μs showed the same polarizations as those under the higher concentration (Figure 3b), though the line width of the sharp peaks are narrower. In the TREPR spectrum at 1.5−1.6 μs, no broad signals were observed, and the sharp signal with a hyperfine-level-dependent

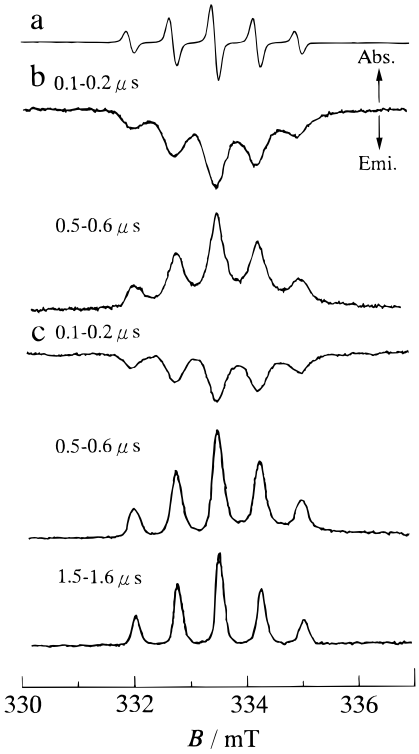

Figure 3. (a) X-band steady-state EPR spectrum of nit-p-py. Time-resolved EPR spectra for the ZnTPP and nit-p-py system; (b) ZnTPP (2 mM) and nit-p-py (5 mM) and (c) ZnTPP (0.5 mM) and nit-p-py (0.5 mM). The gate times are described in the figure.

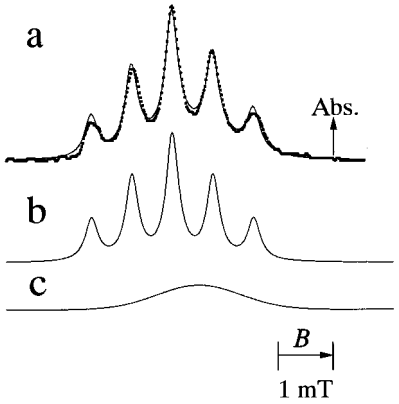

Figure 4. (a) The X-band TREPR spectrum (···) of the ZnTPP (2 mM) and nit-p-py (5 mM) system at 0.5−0.6 μs (Figure 3b) and its simulation (—) with superposition of the two components; (b) the five Lorentzian peaks with the EPR parameters ($g = 2.0068$ and $A_N = 0.74$ mT) of the nit-p-py radical and the broad Gaussian peak with $g = 2.0032$ and $\Delta B_{1/2} = 1.8$ mT.

A/E polarization was distinctly observed together with the net A polarization.

Time profiles of the sharp peak at the lowest field and the broad peak are shown in Figure 5 including a time profile of the optical transient absorption. The time profiles were measured at low concentration of the radical (0.5 mM; Figure 3c) to avoid an overlap of the broad and the sharp signals. In this system, 0.27 mM complex, 0.23 mM free ZnTPP, and 0.23 mM free nit-p-py are in existence. The decay curve of the sharp CIDEP signal was analyzed by a double-exponential function with time constants of 0.37 ± 0.08 and 2.0 ± 0.2 μs for the emissive and absorptive components, respectively. The decay curve of the broad CIDEP signal was analyzed by a triple-exponential function with 0.1 ± 0.08, 0.35 ± 0.08, and 1.9 ± 0.2 μs. The transient absorption observed under the laser

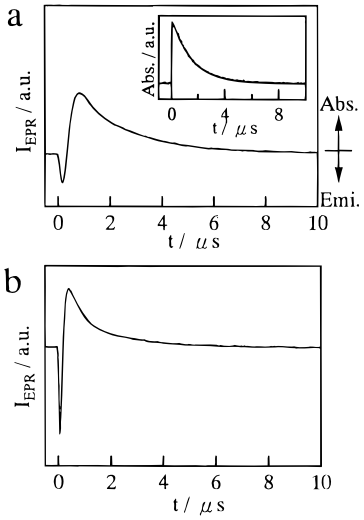

Figure 5. Time profiles of (a) the sharp signal at the lowest-field and (b) the broad signal in the CIDEP spectrum of the ZnTPP (0.5 mM) and nit-p-py (0.5 mM) system. The inset shows the time profile of the T−T absorption of ZnTPP.

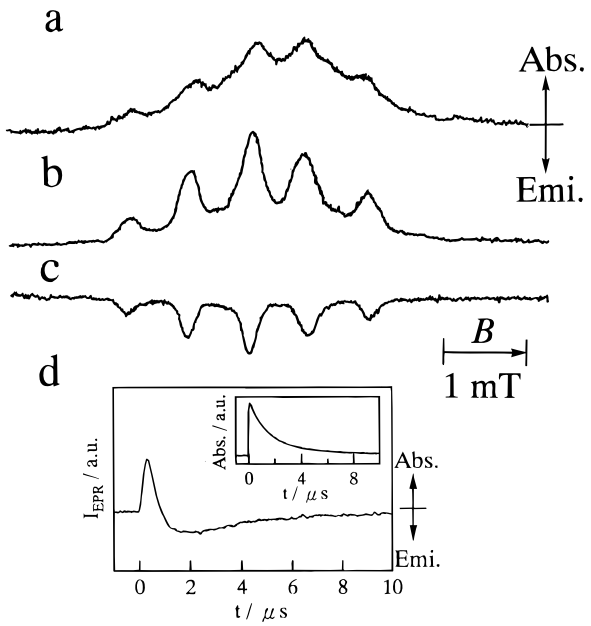

Figure 6. X-band TREPR spectra observed at (a) 0.1−0.2 μs, (b) 0.2−0.3 μs, and (c) 0.5−0.6 μs and (d) time profile of the sharp signal for the ZnTPP (1 mM) and nit-m-py (1 mM) system. The inset shows the time profile of the T−T absorption of ZnTPP.

excitation at 580 nm was assigned to the triplet−triplet (T−T) absorption of ZnTPP from the spectral shape ($\lambda_{max} = 465$ nm) and its excitation spectrum. The decay of the T−T absorption, namely the decay of T_1 ZnTPP, was found to follow a single-exponential function with a time constant of 1.8 ± 0.1 μs. These results indicate that the absorptive polarization of the sharp signal (2.0 ± 0.2 μs) decays with the same time constant as that (1.8 ± 0.1 μs) of T_1 ZnTPP. Since the broad signal having $g = 2.0032$ and $\Delta B_{1/2} = 1.8$ mT was not observed at later times (Figure 3c), the slow component observed at the broad peak is attributed to the signal of thermalized T_1 ZnTPP having a much larger line width ($\Delta B_{1/2} = 9$ mT).[6b,26]

(2). ZnTPP-nit-m-py System. X-band TREPR spectra were observed with the laser excitation at 620 nm in the ZnTPP-nit-m-py system and are shown in Figure 6, where the time profiles of the sharp CIDEP signal and the T−T absorption of ZnTPP are also shown. The sharp ($g = 2.0068 \pm 0.0002$) and broad

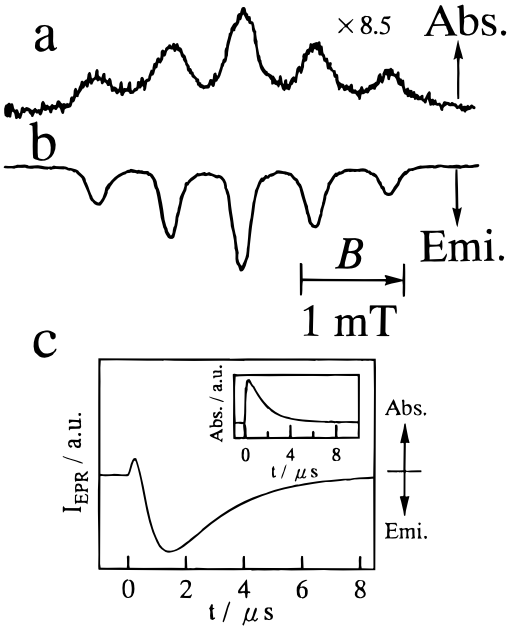

Figure 7. X-band TREPR spectra observed at (a) 0.1−0.2 μs and (b) 1.5−1.7 μs and (c) the time profile of the sharp signal for the ZnTPP (1 mM) and nit-o-py (1 mM) system. The inset shows the time profile of the T−T absorption of ZnTPP.

signals ($g = 2.0023 \pm 0.0005$) were again observed as those in the ZnTPP-nit-p-py system. The CIDEP signals showed absorptive (A) and emissive (E + E/A) polarizations at earlier and later time regions, respectively. These polarizations are just opposite to those obtained for the ZnTPP-nit-p-py system. The decay curves of the sharp CIDEP signal and the T−T absorption of ZnTPP were analyzed by a double-exponential function with the time constant of 0.55 ± 0.08 (absorptive) and 1.5 ± 0.2 μs (emissive) and a single-exponential function with 1.6 ± 0.1 μs, respectively. These results indicate that the slow component of the sharp signal decays with the same time constant of T_1 ZnTPP.

(3). ZnTPP-nit-o-py System. X-band TREPR spectra obtained in the ZnTPP-nit-o-py system are shown in Figure 7 together with time profiles of a sharp CIDEP signal and the T−T absorption of ZnTPP. In this system, only the sharp signal was observed, providing absorptive and emissive polarizations at earlier and later time regions, respectively. The emissive CIDEP signals exhibited a hyperfine-level-dependent E/A polarization, which is of opposite and same phase as those obtained for the nit-p-py and the nit-m-py systems, respectively. The decay curve of the sharp signal was found to be fitted by a double-exponential function with the time constants of 0.61 $\pm$ 0.08 (absorptive) and 1.9 $\pm$ 0.2 μs (emissive). The decay curve of the T−T absorption of ZnTPP was simulated by a single-exponential function with 1.8 $\pm$ 0.1 μs, indicating coincidence in the decay times of the slower component of the CIDEP signal and the T−T absorption. This was also the case in the nit-p-py and nit-m-py systems.

In order to examine an interaction between nit-o-py and metalloporphyrins, 1 M pyridine was added to the nit-o-py system, since most of the porphyrins ligate with pyridine. Although the CIDEP signal with the faster decay was not quenched, the intensity of the signal with the slower decay decreased strikingly. This result indicates that the weak interaction surely occurs between the radical and the porphyrin, as reported in the phenyl−nitronyl nitroxide radical system.[6b]

(4). Other Systems. In the MgTPP-nit-p-py and the MgTPP-nit-m-py systems, X-band TREPR spectra were obtained as shown in Figure 8. The sharp and broad CIDEP signals were observed at $g = 2.0069 \pm 0.0002$ and 2.0038 ± 0.0005, respectively, in both the systems. In the nit-p-py system, both the sharp and broad CIDEP signals have the faster and slower decays, whose polarizations are an emission (E) and an absorption (A) of microwave, respectively. The reverse polarizations of A and E were observed in the nit-m-py system. These polarization patterns are just the same as those in the ZnTPP systems.

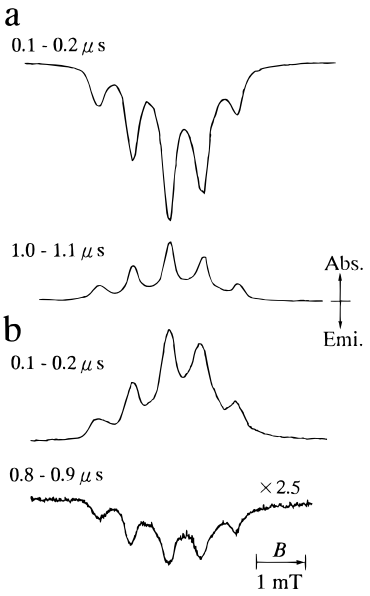

Figure 8. X-band TREPR spectra observed for (a) the MgTPP-nit-p-py and (b) the MgTPP-nit-m-py systems. The gate times are described in the figure.

TABLE 1: The CIDEPs Observed in Systems of Metalloporphyrins and Axial-Ligating Nitroxide Radicals

porphyrins	radicals	sharp (R)[a,b]	broad (Q_1)[a,b]
MgTPP	nit-p-py	E → A	E → A
	nit-m-py	A → E	A → E
	nit-o-py	E → E	
ZnTPP	nit-p-py	E → A	E → A
	nit-m-py	A → E	A → E
	nit-o-py	A → E	
ZnOEP	nit-p-py	E → A	
	nit-m-py	A → E	
	nit-o-py	A → E	

[a] E and A denote an emission and an absorption of microwave, respectively. [b] R and Q_1 stand for the radicals and the excited quartet states, respectively.

The obtained CIDEPs in all systems are summarized in Table 1. From the table, it follows that the observed polarizations of both the sharp and broad signals in the nit-p-py and the nit-m-py systems are independent of the central metal but dependent on the kind of radical. For the nit-o-py system, the first polarizations observed at the earlier time exhibited the same signs of the T_1 polarizations of the corresponding porphyrins. The second later ones provided emissions, which are independent of the kind of porphyrin. From the analyses of the decay curves in all systems, it was found that the first CIDEP signal decays with 0.51 ± 0.15 μs and the second signal arises and decays with 0.51 ± 0.15 μs and a few microseconds, respectively. The slower decay times always agree well with the triplet lifetimes of the porphyrins.

b. W-Band EPR. In order to confirm an existence of the broad signal and determine exactly its EPR parameters of g and $\Delta B_{1/2}$, we carried out time-resolved W-band EPR experiments. Obtained TREPR spectra are shown in Figure 9 for the ZnTPP-

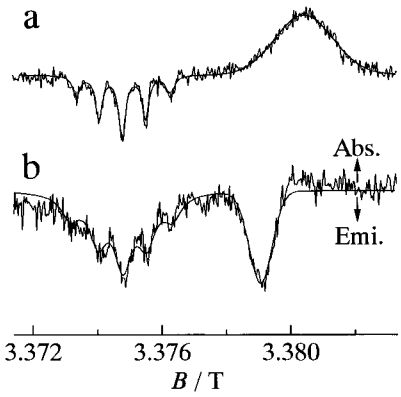

Figure 9. W-band TREPR spectra obtained at 0.01−0.06 μs and 0.05−0.10 μs for (a) the ZnTPP-nit-p-py and (b) the MgTPP-nit-p-py systems, respectively. The solid curves are the spectral simulations using the parameters described in the text.

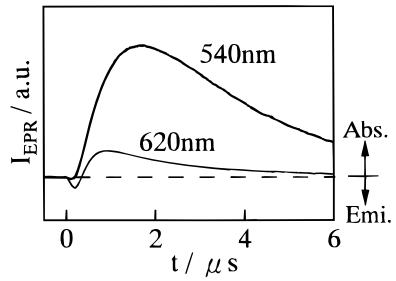

Figure 10. Time profiles of the sharp signals observed at the excitation wavelengths of 540 (thick line) and 620 nm (thin line) for the ZnTPP-nit-p-py system by X-band TREPR.

nit-p-py and the MgTPP-nit-p-py systems. From the figure, it is distinctly found that the TREPR spectra are composed of both sharp and broad components with different g values. These spectra were simulated by the five Lorentzian lines used for the simulation of the X-band EPR spectrum ($g = 2.0068 \pm 0.0002$, $A_N = 0.74 \pm 0.1$ mT, intensity ratio = 1:2:3:2:1) and the broad Gaussian line with the g values of 2.0034 ± 0.0005 for the ZnTPP system and of 2.0042 ± 0.0005 for the MgTPP system. The line width ($\Delta B_{1/2}$) was obtained as 2.0 ± 0.3 and 0.9 ± 0.1 mT for the ZnTPP and MgTPP systems, respectively. Similar experiments were made on the ZnTPP-nit-m-py and the MgTPP-nit-m-py systems. The broad signal was also observed as in the nit-p-py systems and could be simulated by the Gaussian line shape with EPR parameters, $g = 2.0032 \pm 0.0005$ and $\Delta B_{1/2} = 1.4 \pm 0.2$ mT for the ZnTPP system and $g = 2.0043 \pm 0.0005$ and $\Delta B_{1/2} = 1.3 \pm 0.2$ mT for the MgTPP system. From the results, it is found that the g value depends on the central metal of the porphyrin. The line width of the broad signal decreased with the delay time of the gate; $\Delta B_{1/2} = 1.2 \pm 0.2$ mT with the gate time of 10−50 ns and 0.9 ± 0.1 mT with 50−100 ns for the MgTPP-nit-m-py system. This phenomenon is interpreted in terms of a well-known effect that arises from the interaction between the microwave field and the transient magnetization.[27] On the basis of the results obtained by X- and W-band TREPR, it is concluded that the line widths of the broad signals are 1.1 ± 0.3 mT in all systems except for the ZnTPP-nit-p-py system, where the somewhat broader signal was observed.

3. Origin of the CIDEP Signals. The dependence of the CIDEPs on the excitation wavelength was examined in order to elucidate the origin of the polarizations. Figure 10 shows time profiles of the sharp CIDEP signals observed in the ZnTPP (0.5 mM)-nit-p-py (0.5 mM) system with excitations at 540 and 620 nm. Under this condition, 54% ZnTPP ligate with nit-p-py, indicating that three species, ZnTPP, nit-p-py, and the axial-ligating complex, are present with almost the same amounts in this system. As shown in Figure 2, the complex is selectively excited at 620 nm and ZnTPP is excited dominantly at 540 nm. From the time profiles of the ZnTPP-nit-p-py system, it is found that the sharp signal with the faster decay diminishes at the excitation wavelength of 540 nm,[28] whereas the sharp signal with the slower decay increases strikingly. The broad signal is stronger at 600 nm than that obtained at 540 nm. By comparing these results with those of the concentrated radical system (Figure 3b) where the more complexes are existing, it is concluded that the sharp signal having the slower decay is generated from both the complex and free ZnTPP. On the other hand, the broad signal and the sharp signal with the faster decay are not produced from free ZnTPP but from the complex.

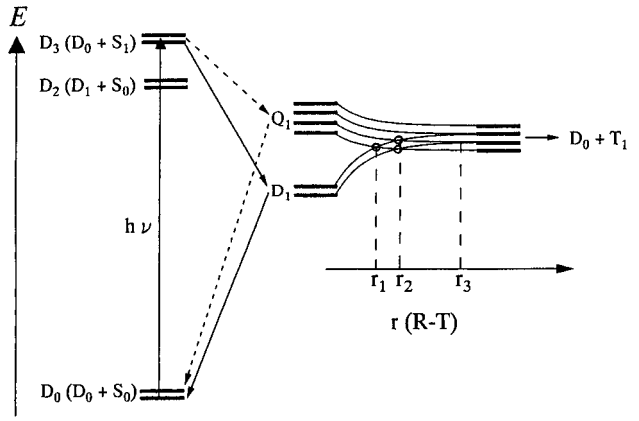

Figure 11. Energy diagram of the radical-ligated porphyrin system under $J < 0$. The solid and dotted lines denote the RTPM with singlet and triplet precursors, respectively.

Discussion

1. Electronic States of the Radical-Ligated Porphyrin. A schematic energy diagram of the RTP system is shown in Figure 11.[29] The exchange interaction between R−T gives rise to excited quartet (Q_1) and doublet (D_1) states, and their splitting ($3J$) varies depending on the distance between the porphyrin and the radical as shown in the figure. On laser excitation, the complex is initially excited to the D_3 state which is composed of D_0 of the radical and S_1 of the porphyrin. The populations of the D_3 state decay via an intersystem crossing (isc) to the $^4(T_1-D_0)$ (named Q_1) state and an internal conversion (ic) to the $^2(T_1-D_0)$ (named D_1) state under the condition that $J \gg |g\beta B|$. The populations of the D_1 state are larger than those of the Q_1 state just after the laser excitation owing to the faster ic compared with the isc and become smaller due to the faster decay to the D_0 state. RTPM polarizations are generated from interactions between the Q_1 and D_1 states with their unequal populations.

2. Assignment of the CIDEP Signal. Both the sharp and broad TREPR signals were observed in the nit-p-py and the nit-m-py systems, and only the sharp signal was observed for the nit-o-py system. The sharp signals provided the same EPR parameters as those of the steady-state EPR signals of the radicals and are assigned to the signals of the ground state (D_0) of the noncoordinated radical and/or the radical-ligated porphyrin.

The broad CIDEP signals were clearly separated at $g = 2.003 \pm 0.001$ for the ZnTPP system and at $g = 2.004 \pm 0.001$ for the MgTPP system by the W-band experiments. It is also indicated that the broad signal is generated by the direct excitation of the complex. Therefore, the signal is considered to come from the excited state of the complex. The g values[12]

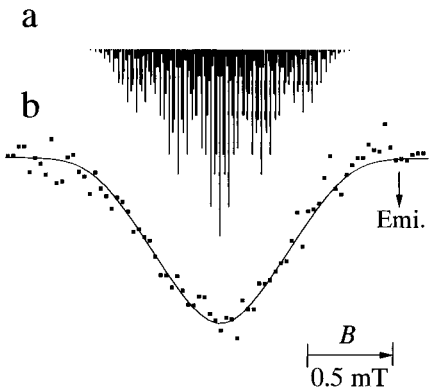

Figure 12. (a) The stick plots of the hyperfine splitting lines expected for the Q_1 state. (b) The dotted and solid curves denote the observed spectrum of the broad signal for the MgTPP-nit-m-py system with W-band TREPR and the simulated spectrum with the line width of 0.2 mT on each hyperfine line, respectively.

of the Q_1 and the D_1 states are expressed as follows, under the condition that the exchange interaction (J) is stronger than the Zeeman interaction ($\sim$0.3 cm^{-1}), the hyperfine coupling ($\sim 10^{-3}$ cm^{-1}), and the zero-field splitting ($\sim 10^{-2}$ cm^{-1}),[12]

$$g(Q_1) = (g_R + 2g_T)/3 \quad (2)$$

$$g(D_1) = -(g_R - 4g_T)/3 \quad (3)$$

The g values of the Q_1 and D_1 states are estimated to be 2.001 $\pm$ 0.003 and 1.995 $\pm$ 0.003, respectively, from eqs 2 and 3 and the g values of T_1 ZnTPP (1.998 $\pm$ 0.003)[16] and nit-p-py (2.0068 $\pm$ 0.0002). The g value (2.003 $\pm$ 0.001) of the broad signal for the ZnTPP system is in good agreement with that of the Q_1 state, which indicates that the broad signal is due to the Q_1 state. For the MgTPP system, although the g value of the T_1 MgTPP was not reported, it is expected that g is closer to that (2.0023) of a free electron than that of T_1 ZnTPP as already shown in the anion radicals of ZnTPP and MgTPP.[32] Then, the g value of the Q_1 state is expected to be larger in the MgTPP system (2.004 $\pm$ 0.001) than that in the ZnTPP system, which is consistent with the result obtained in our system.

The simulation of the line shape was carried out by taking into consideration of contribution from hyperfine splittings. The magnitude of the hyperfine interaction in the Q_1 state is expressed as[8c,33]

$$\langle Q,M_s|H_{hf}|Q,M_s'\rangle = (1/3)(A_R I_z + A_{T_1} I_z + A_{T_2} I_z) M_s \delta_{M_s M_s'} \quad (4)$$

From eq 4, the hyperfine splitting in the Q_1 state is found to be one-third of those in the T_1 and D_0 states. The hyperfine coupling constants are estimated from those of the cation and the anion of ZnTPP, A_N = 0.158 mT ($ZnTPP^+$)[34] and $A_{\beta-H}$ = 0.093 mT ($ZnTPP^-$),[32] and the nitroxide radical, 0.74 mT (nit-p-py), because the unpaired electrons of the Q_1 state are considered to be mostly occupied in the highest occupied molecular orbital (HOMO) and the lowest unoccupied molecular orbital (LUMO) of ZnTPP and the singly occupied molecular orbital (SOMO) of the radical. A typical example of the simulated spectrum is shown in Figure 12, where the observed spectrum agrees well with the simulated one having the Gaussian line width ($\Delta B_{1/2}$) of 0.2 mT on each hyperfine line. The line width (0.2 mT) is considered to come from the unresolved lines due to the weak hyperfine coupling. On the basis of the simulations of both the g value and line width, the broad signal is definitively assigned to that of the Q_1 state of RTP.[35]

There are two kinds of allowed transitions in the Q_1 state, $|Q_1 \pm 3/2\rangle \rightleftarrows |Q_1 \pm 1/2\rangle$ and $|Q_1 + 1/2\rangle \rightleftarrows |Q_1 - 1/2\rangle$. The former transition is expected to provide a much broader spectrum than the latter one due to the zero-field splitting (zfs). The D value of the Q_1 state was already reported as 0.25 GHz from the low-temperature experiment and the molecular orbital (MO) calculation.[12] For T_1 ZnTPP, the TREPR spectrum ($\Delta B_{1/2}$ = 9 mT) was observed in toluene at room temperature and interpreted by slow rotations of molecules giving insufficient averaging of the zfs (D = 0.93 GHz). This is also considered to be the case of the Q_1 spectrum at room temperature.[6b,26] Although the separation ($4D$) of the outermost lines in the Q_1 state is about one-half of that ($2D'$) in the T_1 state, the rotational correlation time of the complex must be longer than that for ZnTPP. The broadening due to incomplete averaging in the $|Q_1 \pm 3/2\rangle \rightleftarrows |Q_1 \pm 1/2\rangle$ transitions is surely much larger than the obtained line width (0.2 mT) of the Q_1 state. From these analyses, it is concluded that the observed broad signal is due to the $|Q_1 + 1/2\rangle \rightleftarrows |Q_1 - 1/2\rangle$ transitions.

3. CIDEP of the Q_1 State. The CIDEP signals of the Q_1 state showed two polarizations with different decay times analogous to the radical signals. The polarizations varied from an emission (E) to an absorption (A) of microwave for the nit-p-py system and A to E for the nit-m-py system, as summarized in Table 1. The signs of the CIDEPs are not dependent on the porphyrin but on the radical. The CIDEPs due to RTPM with singlet (S) and triplet (T) precursors are A and E for $J < 0$ and E and A for $J > 0$, respectively, depending on the sign of J ($H_{ex} = -2J\mathbf{S}_T\cdot\mathbf{S}_D$). The polarization due to the S precursor RTPM decays faster than that due to the T precursor RTPM, because the D_1 state deactivates to D_0 via a prompt internal conversion, as described in section 1. From the results, the first and second CIDEPs of the Q_1 state are attributed to RTPM with S and T precursors, respectively, having different signs of J, positive for the nit-p-py system and negative for the nit-m-py system.

Since the encounter of a radical with a short-lived S_1 molecule is very crucial for RTPM with S precursors, the decay rate of the S_1 state must be comparable or slower than the collision rate. The S_1 lifetimes of the MgTPP,[36a] ZnTPP,[36] and ZnOEP[36b] were reported to be 9.2, 2.7, and 2.5 ns, respectively, which is shorter than the inverse (100 ns) of the collision rate[37] in toluene with [porphyrin] = [radical] = 1 mM. However, in our system such an encounter is not necessary, because the radical-ligated porphyrin is directly excited and the condition of more populations in D_1 than in Q_1 is achieved just after the excitation. Mixings in energy levels of RTP are one of the important requirements for RTPM polarizations. We consider that the metal−ligand vibration occurring in the excited states of the complex leads Q_1 and D_1 to the mixing regions (Figure 11).

The spin-selective isc from the D_3 ($D_0 + S_1$) state to the Q_1 ($D_0 + T_1$) state would produce polarizations on the Q_1 state originating from those of T_1 porphyrins, an absorption for ZnTPP[12] and ZnOEP and an emission for MgTPP. Such polarizations, however, were not actually observed in solution.

4. CIDEP of Radicals. In the nit-p-py and the nit-m-py systems, axial-ligations (eq 1) were shown to occur between the porphyrins and the nitroxide radicals from the shift of the visible absorption spectra (Figure 2). Such a distinct spectral change was not observed for the nit-o-py radical. We analyze the CIDEPs in the nit-p-py and the nit-m-py systems separately from those in the nit-o-py system.

In the nit-p-py and the nit-m-py systems, two kinds of CIDEP signals appeared on the radical in different time regions. The results for the fast component are summarized as follows. (1)

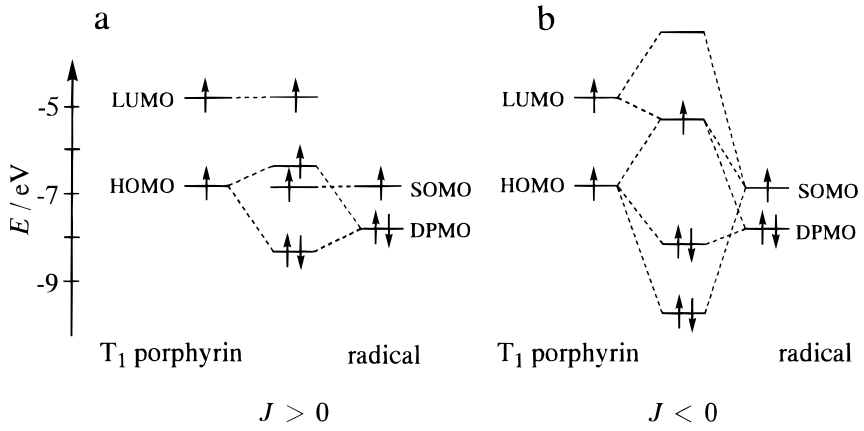

Figure 13. Schematic illustration of interorbital interactions for (a) the nit-p-py and (b) the nit-m-py and the nit-o-py systems. The energies of the MOs of the porphyrin (TPP) and the radical are reported in ref 45.

The polarizations are emissive for the nit-p-py system and absorptive for the nit-m-py system. (2) These signs are in good agreement with those of the corresponding Q_1 states (Table 1). (3) The intensity increases with increasing the excitation of the ligating complex. (4) The decay time (0.51 ± 0.15 μs) of the polarization is the same as the spin−lattice relaxation (SLR) time (τ_1) of the radical ($\tau_1 = 0.6 \pm 0.1$ μs)[6b] within experimental error. The electron spin polarization transfer (ESPT) rate in toluene was reported to be the same as the diffusion rate (1×10^7 s^{-1}) at [TEMPO] = 1 mM, which is comparable to the decay rate (1×10^7 s^{-1}) of the fast polarization of the Q_1 state. These results lead us to conclude that this fast polarization is due to an ESPT from the polarized Q_1 state to the D_0 state of the free radical and/or the complex.[38] As the translational and rotational diffusion rates[39] of the radical are faster than those of the complex and a fast encounter between a polarized donor and an acceptor is important for the ESPT process,[6] the ESPT is considered to occur dominantly to the nonligating radical.

The results for the slower component are summarized as follows. (1) The polarizations are absorptive (A + A/E) for the nit-p-py system and emissive (E + E/A) for the nit-m-py systems, which show the same polarizations due to RTPM with T precursors under positive and negative signs of *J*, respectively. (2) The polarization is generated from both excitations of the axial-ligating complex and the free porphyrin. (3) The rise (0.51 ± 0.15 μs) and decay times of the polarizations are the same as the SLR time (0.6 ± 0.1 μs) of the radical and those of the corresponding T_1 porphyrins, respectively. The T precursor RTPM polarization arises and decays with a SLR time (τ_1) of the radical and a decay time (τ_d) of the T_1 state, respectively, when $\tau_1 < \tau_d$.[6] From these results, the slow component of the polarization is assigned to be due to the RTPM with T precursors. The RTPM is considered to occur in processes of the dissociation of the complex and the encounter of the radical and T_1 porphyrin. The polarization patterns of A + A/E and E + E/A indicate that the sign of the electron exchange parameter *J* is positive for the nit-p-py system and negative for the nit-m-py system, which is in good agreement with the results obtained from the Q_1 polarization described in the previous section. The result that the exchange coupling between the T_1 state and the radical is reversed for the isomeric ligated porphyrins is very interesting and is discussed in the following section.

For the nit-o-py systems, only the sharp signals were observed with two kinds of polarizations; the first polarizations were emissive for the MgTPP system and absorptive for the ZnTPP and the ZnOEP systems, showing the same polarizations as those of the corresponding T_1 porphyrins. The decay time (0.61 ± 0.08) of this polarization was the same as the SLR time (0.6 ± 0.1 μs) of the radical.[6b] The second CIDEP was emissive in all the systems, involving the hyperfine-level-dependent E/A polarization. The decay time of the second polarization was in good agreement with that of each T_1 porphyrin. From these results, the first and second polarizations are attributed to ESPT and RTPM with triplet precursors, respectively, between the T_1 porphyrins and the radicals. *J* is determined to be negative in this system.

5. Electron-Spin Exchange Interaction. In most systems of transient radical pairs in solution, the exchange interaction parameter *J* exhibits a negative sign, since two tumbling radicals have little chance in getting conformations with positive *J* as compared with those with negative *J*.[40] In our system, however, it was demonstrated from the analyses of the RTPM polarizations of both the radical and the Q_1 state that *J* is positive for the nit-p-py system. Here, we discuss why the sign of *J* becomes positive for the nit-p-py system. The energy diagram and the coupling pattern of the possible candidates of our systems are schematically shown in Figure 13. The orbitals involved in the T_1 porphyrin are the HOMO (a_{1u} or a_{2u}) and the LUMO (e_g) of the S_0 porphyrin. For the nit-p-py radical, two types of orbitals should be considered, the SOMO (π^*) orbital localized on the nitroxide moiety[25,41] and the orbitals delocalized over the pyridine ring (DPMO) such as the highest doubly occupied MO.[41]

For the nit-p-py system, the axial ligation at the para position of the pyridine ring makes the direct interactions between the HOMO−LUMO of the porphyrin and the SOMO of the radical much weaker due to their large separation (∼6 Å). The interaction between the HOMO−LUMO and the SOMO through the central metal of the porphyrins and the pyridine is also considered to be less effective, since the spin densities on these parts are very low (∼1%).[25,41,42] On the other hand, the interaction between the HOMO−LUMO of the porphyrin and the DPMO of the radical is enhanced by a close approach via the axial ligation and causes the spins of the unpaired electrons to couple ferromagnetically ($J > 0$) as shown in Figure 13a.[41,43,44]

For the nit-m-py system, the interactions via the direct overlaps of the HOMO−LUMO of the porphyrin and the SOMO of the radical are dominant because of their shorter distance (∼3 Å). These interactions lead us to predict a negative *J* value, which was realized in the experiment. For the nit-o-py system, as the direct overlap of the SOMO of the radical and the HOMO and LUMO of the porphyrin is strong due to the interaction via the oxygen of the radical, *J* becomes negative. These interaction

schemes in the nit-m-py and the nit-o-py systems are demonstrated in Figure 13b.

Conclusion

X- and W-band TREPR studies have been made on electron spin polarizations of radical−triplet pairs (RTP) in systems of excited triplet (T_1) porphyrins and axial-ligating radicals. The TREPR spectra exhibited two kinds of signals in solution at room temperature, which were unambiguously assigned by W-band EPR to those of the ground (D_0) state of the radical and excited quartet (Q_1) state of the RTP. Each signal showed two CIDEP polarizations in different time regions. It was found that the CIDEPs of the Q_1 state with faster and slower decays are due to radical−triplet pair mechanisms (RTPMs) with singlet and triplet precursors, respectively. In the nit-p-py and the nit-m-py systems, the polarizations of the radical were interpreted in terms of an electron spin polarization transfer (ESPT) from the polarized Q_1 state and RTPM. The CIDEPs for the nit-o-py system were explained by ESPT and RTPM with triplet precursors between the T_1 porphyrin and the radical.

The RTPM polarizations provided information about the exchange coupling parameter J between the T_1 porphyrin and the radical: J is positive for the nit-p-py system and negative for the nit-m-py and the nit-o-py systems. The positive J peculiar to the nit-p-py system was explained by consideration of the interaction between the π and π^* orbitals of the T_1 porphyrin and the molecular orbital delocalized over the pyridine ring of the radical.

Acknowledgment. This work was supported by Grant-in-Aid for Scientific Research on International Scientific program (No. 07044058) from the Ministry of Education, Science and Culture, Japan, and by the Deutsche Forschungsgemeinschaft (SFB 337).

References and Notes

(1) (a) Blättler, C.; Jent, F.; Paul, H. *Chem. Phys. Lett.* **1990**, *166*, 375.

(2) Jenks, W. S.; Turro, N. J. *Res. Chem. Intermed.* **1990**, *13*, 237. (b) Turro, N. J.; Khudyakov, I. V.; Bossmann, S. H.; Dwyer, D. W. *J. Phys. Chem.* **1993**, *97*, 1138.

(3) (a) Kawai, A.; Okutsu, T.; Obi, K. *J. Phys. Chem.* **1991**, *95*, 9130. (b) Kawai, A.; Obi, K. *J. Phys. Chem.* **1992**, *96*, 52; *Res. Chem. Intermed*. **1993**, *19*, 865.

(4) (a) Shushin. A. I. *Z. Phys. Chem.* **1993**, *182*, 9. (b) Goudsmit G.-H.; Paul, H. *Chem. Phys. Lett.* **1993**, *208*, 73. (c) Goudsmit G.-H.; Paul, H.; Shushin, A. I. *J Phys. Chem.* **1993**, *97*, 13243.

(5) Zilber, G.; Rozenshtein, V.; Cheng, P.-C.; Scott, L. T.; Rabinovitz, M.; Levanon, H. *J. Am. Chem. Soc.* **1995**, *117*, 10720.

(6) (a) Fujisawa, J.; Ishii, K.; Ohba, Y.; Iwaizumi, M.; Yamauchi, S. *J. Phys. Chem.* **1995**, *99*, 17082. (b) Fujisawa, J.; Ohba, Y.; Yamauchi, S. *J. Phys. Chem. A* **1997**, *101*, 434.

(7) (a) Smith, B. E.; Gouterman, M. *Chem. Phys. Lett*. **1968**, *2*, 517. (b) Eastwood, D.; Gouterman, M. *J. Mol. Spectrosc.* **1969**, *30*, 437. (c) Gouterman, M.; Mathies, R. A.; Smith, B. E. *J. Chem. Phys.* **1970**, *52*, 3795. (d) Kim, D.; Holten, D.; Gouterman, M. *J. Am. Chem. Soc*. **1984**, *106*, 2793. (e) Yan, X.; Holten, D. *J. Phys. Chem.* **1988**, *92*, 5982.

(8) (a) van Dorp, W. G.; Canters, G. W.; van der Waals, J. H. *Chem. Phys. Lett.* **1975**, *35*, 450. (b) van Dijk, N.; van der Waals, J. H. *Mol. Phys.* **1979**, *38*, 1211. (c) van der Poel, W. A. J. A.; Nuijs, A. M.; van der Waals, J. H. *J. Phys. Chem.* **1986**, *90*, 1537.

(9) Brugman, C. J. M.; Rettschnick, R. P. H.; Hoytink, G. J. *Chem. Phys. Lett.* **1971**, *8*, 263.

(10) Kothe, G.; Kim, S. S.; Weissman, S. I. *Chem. Phys. Lett.* **1980**, *71*, 445.

(11) Corvaja. C.; Maggini, M.; Prato, M.; Scorrano, G.; Venzin, M. *J. Am. Chem. Soc.* **1995**, *117*, 8857.

(12) Ishii, K.; Fujisawa, J.; Ohba, Y.; Yamauchi, S. *J. Am. Chem. Soc.* **1996**, *118*, 13079.

(13) (a) Faulkner, L. R.; Bard, A. J. *J. Am. Chem. Soc*. **1969**, *91*, 6497. (b) Schulten, K. J. *J. Chem. Phys.* **1984**, *80*, 3668.

(14) Yamauchi, S.; Matsukawa, Y.; Ohba, Y.; Iwaizumi, M. *Inorg. Chem*. **1996**, *35*, 2910.

(15) (a) Levanon, H.; Regev, A.; Galili, T.; Hugerat, M.; Chang, C. K.; Fajer, J. *J. Phys. Chem.* **1993**, *97*, 13198. (b) Levanon, H. *Rev. Chem. Intermed.* **1987**, *8*, 287.

(16) Ishii, K.; Ohba, Y.; Iwaizumi, M.; Yamauchi, S. *J. Phys. Chem.* **1996**, *100*, 3839.

(17) Adler, A. D.; Longo, F. R.; Finarelli, J. D.; Goldmacher, J.; Assour, J.; Korsakoff, L. *J. Org. Chem.* **1967**, *32*, 476.

(18) Adler, A. D.; Longo, F. R.; Kampas, F.; Kim, J. B. *J. Inorg. Nucl. Chem.* **1970**, *32*, 2443.

(19) Lindsey, J. S.; Woodford, J. N. *Inorg. Chem.* **1995**, *34*, 1063.

(20) Caneshi, A.; Gatteschi, D.; Rey, P. *Prog. Inorg. Chem.* **1991**, *39*, 331.

(21) (a) Prisner, T. F.; Rohrer, M.; Möbius, K. *Appl. Magn. Reson.* **1994**, *7*, 167. (b) Prisner, T. F.; van der Est, A.; Bittl, R.; Lubitz, W.; Stehlik, D.; Möbius, K. *Chem. Phys. Lett.* **1995**, *194*, 361.

(22) Miller, J. R.; Dorough, G. D. *J. Am. Chem. Soc.* **1952**, *74*, 3977.

(23) The phosphorescence spectrum observed for the ZnTPP-nit-o-py system showed a red-shifted component at $\lambda = 794$ nm with respect to that ($\lambda = 772$ nm) of ZnTPP. The magnitude of the shift (22 nm) is very close to those (24 ± 2 nm) observed for the radical-complexed ZnTPPs in the ZnTPP-nit-p-py and the ZnTPP-nit-m-py systems, indicating the ligation occurring in the nit-o-py system.

(24) The A_N value was reported to be positive for the analogous radicals.[25]

(25) (a) Zheludev, A. Z.; Barone, V.; Bonnet, M.; Delley, B.; Grand, A.; Ressouche, E.; Rey, P.; Subra, R.; Schweizer, J. *J. Am. Chem. Soc.* **1994**, *116*, 2019. (b) Yamanaka, S.; Kawakami, T.; Yamada, S.; Nagao, H.; Nakano, M.; Yamaguchi, K. *Chem. Phys. Lett.* **1995**, *240*, 268.

(26) Fujisawa, J.; Ohba, Y.; Yamauchi, S. Submitted to *J. Am. Chem. Soc.*

(27) McLauchlan, K. A. *Modern Pulsed and Continuous-Wave Electron Spin Resonance*; Kevan, L., Bowman, M. K., Eds.; Wiley: New York, 1990; Chapter 7.

(28) The decrease of the emissive polarization of the fast component is also originated from ESPT of the absorptive polarization of T_1 ZnTPP.

(29) From the visible absorption spectra, the energy of the D_1 state of the nitronyl nitroxide radical was obtained to be around 14 000 cm^{-1}. The energies of the S_1 and the T_1 states of the porphyrins were reported as ca. 17 000 cm^{-1} [30] and 11 000∼13 000 cm^{-1},[14,31] respectively.

(30) Dorough, G. D.; Miller, J. R.; Huennekens, F. M. *J. Am. Chem. Soc.* **1951**, *73*, 4315.

(31) (a) Harriman A. *J. Chem. Soc., Faraday Trans. 1* **1980**, *76*, 1978. (b) Ohno, O.; Kaizu, Y.; Kobayashi, H. *J. Chem. Phys.* **1985**, *82*, 1779.

(32) Seth, J.; Bocian, D. F. *J. Am. Chem. Soc.* **1994**, *116*, 143.

(33) Bencini, A.; Gatteschi, D. *EPR of Exchange Coupled Systems*; Springer-Verlag: Berlin, 1990; Chapter 3.

(34) Fajer, J.; Borg, D. C.; Forman, A.; Dolphin, D.; Felton, R. H. *J. Am. Chem. Soc*. **1970**, *92*, 3451.

(35) From the obtained g values of the Q_1 states, the isotropic g values of T_1 ZnTPP and T_1 MgTPP are estimated to be 2.001 and 2.003, respectively, by using eq 2.

(36) (a) Harriman, A. *J. Chem. Soc., Faraday Trans. 2* **1981**, *77*, 1281. (b) Rodriguez, J.; Kirmaier, C.; Holten, D. *J. Am. Chem. Soc.* **1989**, *111*, 6500.

(37) The diffusion rate in toluene at room temperature is reported to be 1×10^{10} M^{-1} s^{-1}.[6b]

(38) The difference between the observed decay time of the first polarization and the reported SLR time of the radical is considered to originate from the overlapping contribution of the broad signal.

(39) The translational and rotational diffusion rates are propotional to the inverse of r and r^3, respectively, where r is the radius of the hydrodynamic spherical molecule.

(40) Salikhov, K. M.; Molin, Y. N.; Sagdeev, R. Z.; Buchachenko, A. L. *Spin Polarization and Magnetic Effects in Radical Reactions*; Elsevier: Amsterdam, 1984.

(41) (a) Awaga, K.; Inabe, T.; Maruyama, Y. *Chem. Phys. Lett.* **1992**, *190*, 349. (b) Awaga, K.; Inabe, T.; Nagashima, U.; Maruyama, Y. *J. Chem. Soc., Chem. Commun.* **1989**, 1617.

(42) Davis, M. S.; Morokuma, K.; Kreilick, R. W. *J. Am. Chem Soc.* **1972**, *94*, 5588.

(43) Miller, J. S.; Epstein, A. J. *Angew. Chem., Int. Ed. Engl.* **1994**, *33*, 385.

(44) Kahn, O. *Molecular Magnetism*; VCH: New York, 1993.

(45) (a) Gouterman, M. In *The Porphyrins*; Dolphin, D., Ed.; Academic Press: New York, 1978; Vol. III, pp 1−165. (b) Awaga, K.; Yokoyama, T.; Fukuda, T.; Masuda, S.; Harada, Y.; Maruyama, Y.; Sato, N. *Mol. Cryst. Liq. Cryst.* **1993**, *232*, 27.